

Hydrogen insertion in Ti_2AlC and its influence on the crystal structure and bonds

Q. Liu, H. M. Ding*, B. Q. Du, K. Y. Chu, Y. Shi

School of Energy Power and Mechanical Engineering, North China Electric Power University, Baoding 071003, China

received October 9, 2016; received in revised form January 11, 2017; accepted March 14, 2017

Abstract

First-principles calculations have been performed to study hydrogen insertion in Ti_2AlC and its influence on the crystal structure and bonds. It has been found that H insertion in interstitial sites of the Ti-Al layers is thermally favorable and H diffusion along the basal plane is feasible. When H is inserted into tetrahedral interstitial sites (I_{tet-2}) surrounded by three Ti atoms and one Al atom, the surrounding Ti-Al bonds will be substituted by H-Al and H-Ti bonds. When H is inserted into hexagonal interstitial sites (I_{hexa-5}) surrounded by three Al and two Ti atoms, the Ti-Al bonds will be weakened while H-Ti bonds will be formed, at the same time, surrounding Al-Al bonds will be substituted by H-Al bonds, which will result in a change of part of the crystal structure of the Al layers. In comparison, H insertion into octahedral interstitial sites (I_{oct-3}) surrounded by three Ti and three Al atoms has the least influence on the Ti-Al bonds. As a result, H insertion into I_{tet-2} will seriously weaken the bonding between the Ti and Al layers while H insertion into I_{hexa-5} and I_{oct-3} will enhance it. It is considered that the influence of H on the properties of Ti_2AlC closely depends on its insertion position.

Keywords: MAX phases, Ti_2AlC , first-principles calculations.

I. Introduction

MAX phases ($M_{n+1}AX_n$, where $n = 1, 2$ or 3 , M is an early transition metal, A is an A-group element, and X is either carbon or nitrogen) have a remarkable combination of attractive properties of both metals and ceramics, such as high bulk modulus, corrosion resistance, high electrical and thermal conductivities, crack-healing ability, and easy machinability, etc.¹⁻⁵. Therefore, they have promising applications in various fields, such as high-temperature structural components⁶⁻⁸, solid lubricant materials⁹, structural and fuel coating applications in future fission and fusion reactors¹⁰, and so on. Based on their unique properties and potential applications, numerous works have been performed to study properties of MAX phases. Among them, a large number of works have focused on the influence of doping on properties, including doping in M site, A site or X site. Z.M. Li¹¹ found that the doping of Al could improve the microwave dielectric properties of Ti_3SiC_2 , E.D. Wu *et al.*¹² and H.B. Zhang *et al.*¹³ reported that the doping of 10 at% Al in Ti_3SiC_2 could form $Ti_3Si_{0.9}Al_{0.1}C_2$ and improve its oxidation resistance, while X.L. Xu's work¹⁴ indicated that increased Al content in $Ti_3Si_{(1-x)}Al_xC_2$ would lower its density and hardness. T. Cabioch *et al.*¹⁵ found that the thermal expansion of the c-axis increased with doping of Ge in Cr_2AlC . S. Aryal *et al.*¹⁶ reported that the formation of $Ti_2Al(C_xN_{1-x})$ based on N doping in Ti_2AlC would in-

fluence the mechanical properties, such as bulk modulus, shear modulus and Young's modulus.

Besides M, A and X sites, the interstices are also possible sites for doping, especially for small-size atoms. For example, J.R. Xiao *et al.*¹⁷ reported that He atoms preferred to be doped in the interstitial sites in the Al layer of Ti_3AlC_2 . Zhang HF *et al.* and L.X. Jia *et al.*^{18,19} have studied the doping of He in interstitial sites of Ti_3SiC_2 and found that He could provoke the fracture failure of Ti_3SiC_2 . Besides He, it is known that H can also be easily doped in many solids owing to its smaller size, and the doping of H usually causes the properties of materials, especially metals, to deteriorate by inducing embrittlement. Nevertheless, H.F. Zhang *et al.* and X.D. Ou *et al.*^{20,21} reported that the mechanical response of Ti_3SiC_2 to H seemed to be different from the metals, and the cleavage fracture of Ti_3SiC_2 would not be obviously affected by the doping of H. In order to examine the feasibility of MAX phases for use in hydrogen storage, the doping of H in Ti_3AlC_2 phases has also been studied in our recent work, and it has been found that H can be doped and diffused in Ti-Al layers of Ti_3AlC_2 ²². However, the influence of H doping on the properties of Ti_3AlC_2 has not been discussed in that work.

Considering the different bonding characteristics between H-Al and H-Si, the influence of H doping in $M_{n+1}AlX_n$ phases may be different from that in $M_{n+1}SiX_n$ phases. Therefore, in this work, first-principles calculations have been performed to study H insertion into Ti_2AlC and its influence on the crystal structure and bonds

* Corresponding author: dinghaimin@ncepu.edu.cn

in order to further clarify the effects of H doping on the properties of MAX phases. As we know, there are mainly three kinds of MAX phases, which are 211, 312 and 413 phases. The 211 phase Ti_2AlC is selected as the object of this study rather than 312 or 413 phases for the following reasons. As mentioned above, H atoms prefer to be doped in M-A layers of the MAX phases. In 211 MAX phases, the neighboring two A layers are separated by two M layers while they are separated by three and four M layers in 312 and 413 phases, respectively. In other words, 211 phases have the largest M-A layers numbers per unit weight among all the MAX phases. Therefore, it is deduced that the influence of H on 211 MAX phases should be more remarkable than that on 311 and 413 MAX phases.

II. Calculation Methods

The calculations are based on the density-functional theory and performed using the program package CASTEP. Although the generalized gradient approximation (GGA) is commonly considered to be better than local density approximation (LDA) for studying many aspects, such as the bulk properties of materials²³, it has been found that the calculation results of LDA are in better agreement with experimental data in studying of the hydrogen insertion in solids²⁴. Therefore, local density approximation (LDA) was utilized for structure optimization and energy calculation in this work. Ti_2AlC crystallizes in a hexagonal structure with space group of P63/mmc, as shown in Fig. 1. The lattice constants of Ti_2AlC are set as $a = 2.968 \text{ \AA}$ and $c = 13.224 \text{ \AA}$ according to the work of A. Bouhemadou *et al.*²⁵. The atomic positions of Ti correspond to the 4f, Al to 2b, and C to the 2a. The $3 \times 3 \times 1$ supercell which contains 72 atoms is investigated in this

work. During the calculations, all the atoms in the supercell are fully relaxed. Ultrasoft pseudopotentials (USP) are chosen, the plane-wave cut-off energy of 550 eV is employed after the convergence test and the self-consistent field (SCF) tolerance was set to $5.0 \times 10^{-7} \text{ eV/atom}$. In addition, Mulliken overlap population analysis is also performed in all the calculations, which offers the bond populations in the crystals, and the grids of K-points are sampled by $6 \times 6 \times 4$.

The formation energies of H atoms insertion in different sites in Ti_2AlC are calculated with

$$E_f = E_{\text{tot}}^{n\text{H}} - E_{\text{tot}} - n \frac{E^{\text{H}_2}}{2} \quad (1)$$

where n is the number of H atoms, $E_{\text{tot}}^{n\text{H}}$ is the total energy of the system doped with n H atoms, E_{tot} is the total energy of Ti_2AlC , and E^{H_2} is the total energy of the hydrogen molecule²⁶.

For studying the diffusion of H, the linear synchronous transit (LST) optimization method is used. It is known that the LST optimization method is usually used to find the transition state of a reaction. In this work, the structure with H in the initial position is considered as the reactant and the structure with H in the final position is the product. During the transition-state-structure research, a series of single-point energy calculations are performed on a set of linearly interpolated structures between the reactant and the product. The maximum energy structure along this path provides a first estimate of the transition state structure. Then, an energy minimization in directions conjugate to the diffusion pathway is performed²⁷. This yields a structure closer to the true transition state, which can be used to determine the energy barrier of the diffusion process.

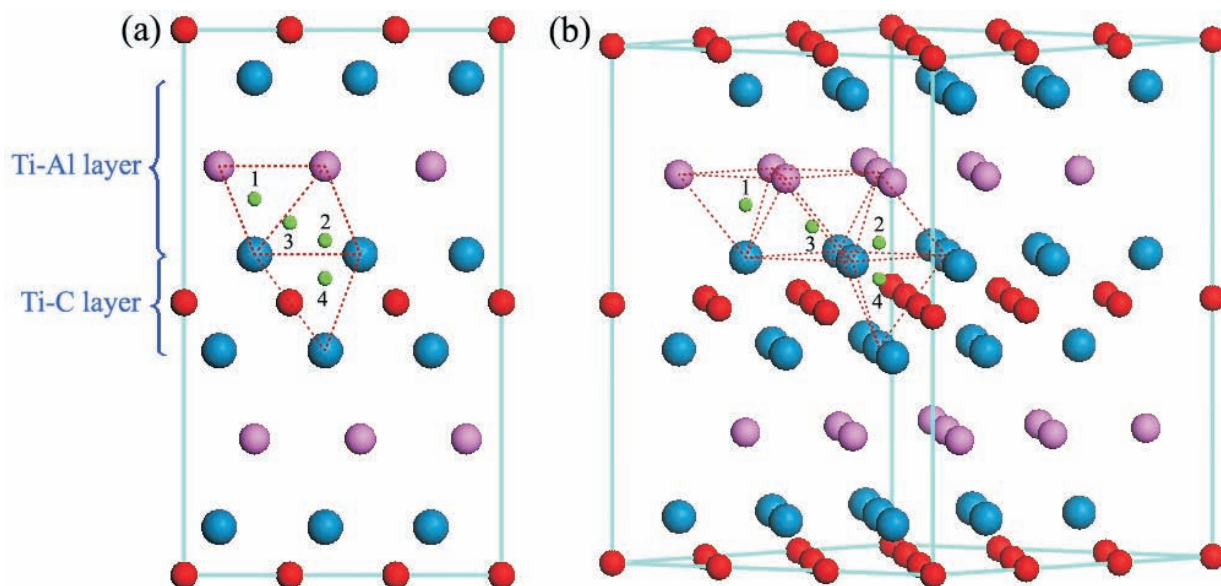


Fig. 1: Crystal structure of Ti_2AlC and interstitial sites considered in this work (a) front view; (b) side view. Small red spheres represent C atoms, large blue spheres represent Ti atoms and purple spheres represent Al atoms, H atoms are denoted by small green spheres. The dash lines are just used to show the positions of H.

III. Results and Discussion

Ti_2AlC phases have a layered hexagonal structure with space group $P63/mmc$, and they consist of alternating layers of Al and Ti_6C octahedron, while C atoms are located in an octahedral Ti atoms coordination²⁸. Therefore, there is a variety of high-symmetry interstitial sites in Ti_2AlC , and these sites can fall into two categories: the interstices in Ti-Al layers and those in compact Ti-C layers, as Fig. 1 shows. Although the actual positions for hydrogen insertion in Ti_2AlC are uncertain based on the experiment results, considering the size of H and its insertion in other materials, the interstitial sites are used as original sites for H insertion into Ti_2AlC during the calculation in this work. Then the original configurations are relaxed to find the lowest energy configurations that can be used to determine the actual preferred positions for H insertion. For Ti-Al layers, there are three kinds of possible interstitial sites for H insertion: the tetrahedral interstitial site denoted as $I_{tetra-1}$ is surrounded by three Al atoms and one Ti atom, the tetrahedral interstitial site $I_{tetra-2}$ is surrounded by three Ti atoms and one Al atom, and the octahedral interstitial site I_{oct-3} is surrounded by three Ti atoms and three Al atoms. They are illustrated as number 1, 2 and 3, respectively in Figs. 1a and b. For Ti-C layers, given C atoms have occupied the octahedral interstitial sites, only the tetrahedral interstitial site formed by Ti atoms which is designated as $I_{tetra-4}$ is considered to be the original site for H insertion during the calculation. It is illustrated as number 4 in Fig. 1.

The formation energies for H insertion into different interstices are calculated with Equation (1) and the results are shown in Table 1. It can be seen that the formation energies for all interstitial sites in Ti-Al layers are negative, indicating that it is thermally favorable for H insertion into Ti-Al layers. Among all the interstitial sites, $I_{tetra-2}$ is the most preferred position with the H insertion energy of -0.58 eV and the next one is I_{oct-3} . However, the difference in the formation energies between these two sites is only 0.05 eV. The formation energy for H insertion into the $I_{tetra-1}$ site is -0.38 eV, indicating that H insertion into $I_{tetra-1}$ is thermally less favorable. In Ti-C layers, it is noticed that H cannot stay stable at the $I_{tetra-4}$ site and will move to an adjacent $I_{tetra-2}$ site after the relaxation. This further confirms that H atoms will not be inserted into M-X layers but prefer to be inserted in M-A layers as found in the previous works^{20,22}.

Table 1: Formation energies for H insertion in different interstices of Ti_2AlC .

Sites for H insertion	Ti-Al layer			Ti-C layer
	$I_{tetra-1}$	$I_{tetra-2}$	I_{oct-3}	$I_{tetra-4}$
E_f (eV)	-0.38	-0.58	-0.53	unstable

The relaxed structures of H insertion in different sites of Ti-Al layers are shown in Fig. 2. It can be seen from Fig. 2a that, actually, H at $I_{tetra-1}$ in original configuration moves to the Al layer after the optimization, and is lo-

cated in the hexagonal interstice surrounded by three Al atoms and two Ti atoms (this interstice will be designated as I_{hexa-5} in the following sections). The bond populations and bond lengths shown in Table 2 demonstrate that H simultaneously bonds with Ti and Al atoms to form covalent bonds, and H-Al bond is stronger than H-Ti bond, as shown in Fig. 2d. It is interesting to note that the bonding between the three Al atoms and the two Ti atoms surrounding the H atom will be changed remarkably after H insertion in I_{hexa-5} . In the Al layer, the surrounding Al-Al bonds will be substituted by H-Al bonds. According to these results, it can be deduced that, if H atoms can insert into all I_{hexa-5} sites in Al layers, the structure of Al layers will be changed from Fig. 3a in which Al atoms form a closed-packed hexagon to Fig. 3b in which H and Al atoms form a hexagon structure that is similar to that of C layer in graphite. However, owing to the impossibility of H insertion into all the hexagonal interstitials, only part of the crystal structure changed into the structure shown in Fig. 3b is possible. At the same time, it is also found from Table 2 that the bond populations of Al-Ti bonds will be decreased from 0.33 to 0.22, which indicates that the strength of the surrounding Al-Ti bonds will be weakened after H insertion into I_{hexa-5} . However, the newly formed H-Ti bonds can offset the weakness of Al-Ti bonds. As a result, it is considered that H insertion into I_{hexa-5} will enhance the bonding between Al and Ti layers.

For H insertion into $I_{tetra-2}$, its relaxed position is close to the center of $I_{tetra-2}$ as shown in Fig. 2b. The bonds shown in Fig. 2e and the bond populations in Table 2 demonstrate that H and Al atoms are bonded to form strong covalent bond. For H-Ti bonds, the bond populations are -0.03, indicating that H bonds with the three surrounding Ti atoms to form weak ionic bonds. At the same time, the surrounding Ti-Al bonds disappear. In addition, unlike H insertion into I_{hexa-5} , H insertion into $I_{tetra-2}$ will not change the structure of the Al layer. Therefore, if all $I_{tetra-2}$ positions are occupied by H atoms, the structure and bonding of Al layers should be changed into Fig. 3c and d. Although the single H-Al bond in Fig. 3c and d is stronger than the original Ti-Al bond, the number of broken Ti-Al bonds is three times that of the newly formed H-Al bonds. As a result, it is considered that the bonding between Al layers and Ti layers will be seriously weakened after insertion of H into $I_{tetra-2}$.

For the H atom at I_{oct-3} , it is almost relaxed to the interstice center and bonds with all the surrounding Ti and Al atoms as shown in Figs. 2c and f. In this case, H-Ti bonds are a little stronger than H-Al bonds as the bond populations in Table 2 shows. Although the strength of the Ti-Al bonds is also weakened by H insertion, the degree of this weakening is much smaller than that caused by H insertion into I_{hexa-5} and $I_{tetra-2}$. Therefore, H insertion into I_{oct-3} will have the least influence on the Ti-Al bonds. At the same time, the surrounding Al atoms will move out and the bonding between them will disappear. Considering the newly formed H-Ti and H-Al bonds, it is deduced that H insertion into I_{oct-3} will also enhance the bonding between Al and Ti layers.

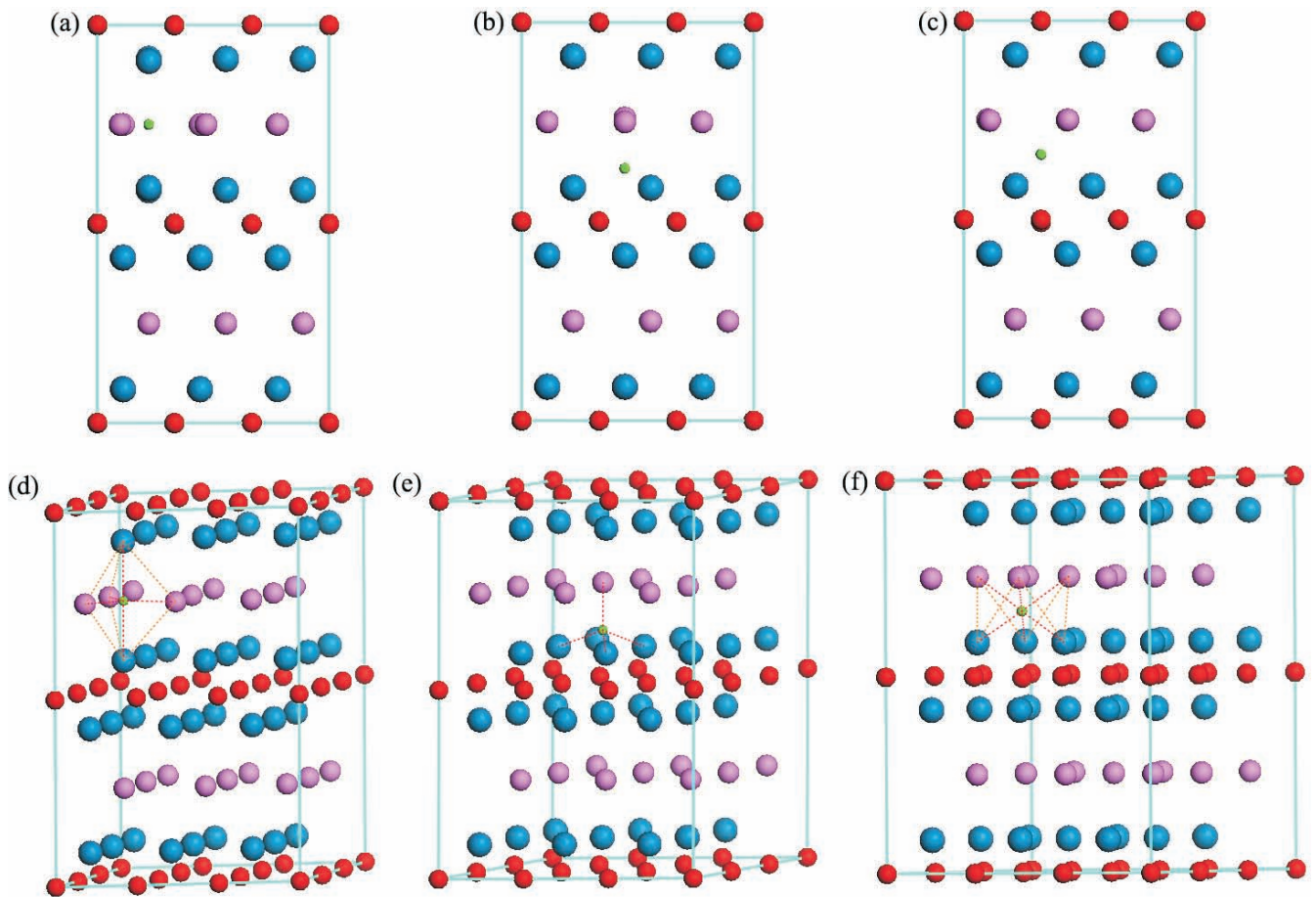


Fig. 2: Lowest-energy positions for H insertion in Ti_2AlC and the bonds surrounding the H atom (a, d) H insertion in $I_{\text{hexa-5}}$; (b, e) H insertion in $I_{\text{tetr-2}}$; (c, f) H insertion in $I_{\text{oct-3}}$. Small red spheres represent C atoms, large blue spheres represent Ti atoms and purple spheres represent Al atoms, H atoms are denoted by small green spheres and dash lines represent the bonds surrounding the H atom.

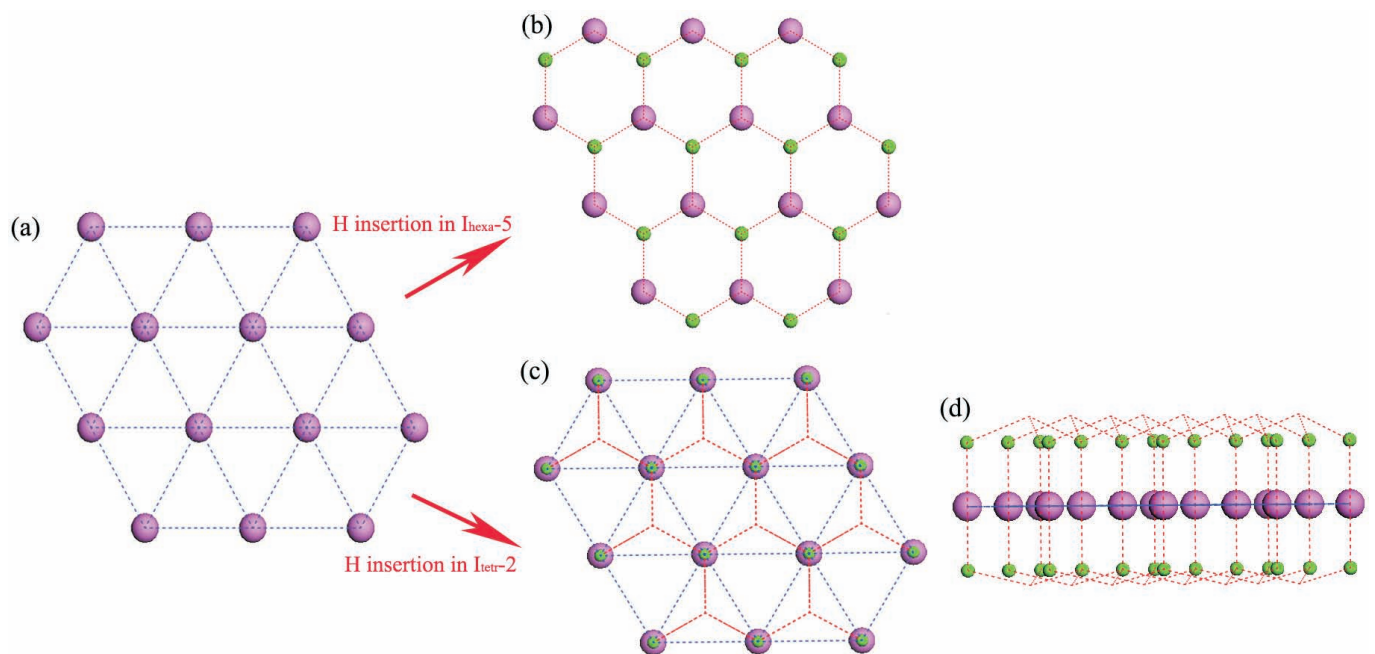


Fig. 3: Schematic diagram of the structure and bond change of Al layers if H atoms are inserted in all the $I_{\text{hexa-5}}$ or $I_{\text{tetr-2}}$ sites in Ti_2AlC (a) structure and bonds of Al layers in Ti_2AlC ; (b) structure and bonds of Al layers after H insertion in $I_{\text{hexa-5}}$; (c, d) structure and bonds of Al layers after H insertion in $I_{\text{tetr-2}}$: top and side view.

Table 2: Bond populations and lengths (Å) for bonds surrounding the H atom in the Ti-Al layer.

Configurations	Bond populations (lengths)			
	Al-Ti	Al-Al	H-Ti	H-Al
Virgin slab	0.33 (2.773)	0.15 (2.968)	–	–
Fig. 2a and d	0.22 (2.844)	Broken	0.14 (2.108)	0.22 (1.908)
Fig. 2b and e	Broken	0.18 (2.975)	-0.03 (1.848)	0.45 (1.673)
Fig. 2c and f	0.30 (2.796)	Broken	0.15 (1.983)	0.09 (2.121)

It has been well acknowledged that the properties of solid materials correlate closely to crystal structure, electronic structure and bonding properties as well²⁹. For MAX phases, they usually have strong covalent bonding between M and X, and relatively weak bonding between M and A³⁰. The M-X blocks contribute more to the high-temperature strength and structural stability¹⁸, while A layers will be easily moved owing to the weak bonding between A and M layers, which contributes to many properties, such as the damage tolerance, self-lubricating property, micro-scale plastic deformation, fracture properties, and so on^{29, 31–34}. For example, it has been reported that the low hardness of Ti_2AlC and Ti_3AlC_2 can be understood based on an easy basal plane slip derived from the layered structure and the relatively weak coupling between TiC slabs and Al planes²⁹. N.I. Medvedeva *et al.*³² also suggested that the weak bonding between Ti and Si layer in Ti_3SiC_2 favors plasticity. And by studying the cleavage fracture in Ti_3SiC_2 , N.I. Medvedeva *et al.*³³ further confirmed that the cleavage fracture in Ti_3SiC_2 tends to occur between Ti and Si layers. Based on their works and the above results, it can be deduced that H insertion should not obviously influence the high-temperature strength of Ti_2AlC owing to its unfavorable insertion in Ti-C layers. On the other hand, its influence on the properties related to Ti-Al layers depends on the position of H insertion. If H atoms are inserted into $I_{tetra-2}$, like He insertion in Ti_3SiC_2 as reported by X.F. Zhang *et al.*¹⁸, it is considered that the fracture failure of Ti_2AlC will be provoked owing to the obvious weakness of the bonding between Al and Ti layers, and Young's modulus and hardness will correspondingly decrease. However, the properties attributed to the weak bonding between Ti and Al layers, such as the self-lubricating property, will be improved. Contrary to H insertion into $I_{tetra-2}$, H insertion into I_{hexa-5} and I_{oct-3} will enhance the properties related to the strong bonding between Al and Ti layers.

According to all the results above, it can be seen that controlling the position of H insertion is essential for regulating its influence on the properties of Ti_2AlC , while the diffusion of H is important for the process. Therefore, in the following section, H diffusion is studied based on the LST optimization method. As mentioned above, H will mainly be inserted into Ti-Al layers of Ti_2AlC . Therefore, the diffusion of H into Ti-Al layers is only considered in this study. And two cases are considered: H diffusion along the basal plane and the c-axis, respectively. On the basis of the results shown in Table 1 and Fig. 2, the diffusion paths along the basal plane are set as following: H firstly diffus-

es from a I_{hexa-5} site to an adjacent I_{oct-3} site (designated as Path I), then it diffuses from the I_{oct-3} site to an adjacent $I_{tetra-2}$ site (designated as Path II). Finally, it diffuses from the $I_{tetra-2}$ site to an adjacent I_{hexa-5} site (designated as Path III). The whole paths are shown in Fig. 4a and the calculated results are shown in Fig. 4b. For diffusion of H along the c-axis, the most possible path should be the diffusion from a I_{oct-3} site to an adjacent I_{oct-3} site as Fig. 4a shows (designated as Path IV), and the results are shown in Fig. 4c.

For H diffusion along the basal plane, it can be seen from Fig. 4b that the energy barrier for diffusion from a I_{hexa-5} site to an adjacent I_{oct-3} site is 0.53 eV, whereas the opposite path should be 0.69 eV according to the results in Table 1. The diffusion of H from I_{oct-3} site to an adjacent $I_{tetra-2}$ site is easier with the energy barrier of 0.36 eV, while the opposite path is also easy with the energy barrier of 0.41 eV. However, it is noticed that the diffusion between a $I_{tetra-2}$ site and a I_{hexa-5} site is difficult. The energy barrier for H diffusion from a $I_{tetra-2}$ site to an adjacent I_{hexa-5} site is 1.08 eV and the opposite path is 0.87 eV. Therefore, it is considered that H diffusion along the basal plane should have mostly occurred between $I_{tetra-2}$ sites and I_{oct-3} sites, while once doped in I_{hexa-5} sites, H atoms will be trapped in the interstices. It has been reported that the activation energy of H diffusion in α -Ti is 0.51 eV according to X.L. Han's work³⁵, and the experimental studies by R.J. Wasilewski *et al.*³⁶ and T.P. Papazoiglou *et al.*³⁷ gave even higher activation energy of 0.54 and 0.64 eV, respectively. It can be seen that H diffusion along the basal plane between $I_{tetra-2}$ sites and I_{oct-3} sites in Ti_2AlC is easier than that in α -Ti. This result is in agreement with the finding of H diffusion in Ti_3AlC_2 in which H diffuses even much more easily along the basal plane in Ti-Al layers owing to the less compact structure of Ti_3AlC_2 ²².

For H diffusion along the c-axis, it is found from Fig. 4c that the energy barrier from a I_{oct-3} site to an adjacent I_{oct-3} site (Path IV) is 1.06 eV, which is larger than that from a I_{oct-3} site to an adjacent I_{hexa-5} site and then to another adjacent I_{oct-3} site (this path is shown in Fig. 4a by red dash line and designated as Path V). Therefore, Path V is more possible than Path IV for H diffusion along the c-axis but the diffusion is still more difficult than that along the basal plane.

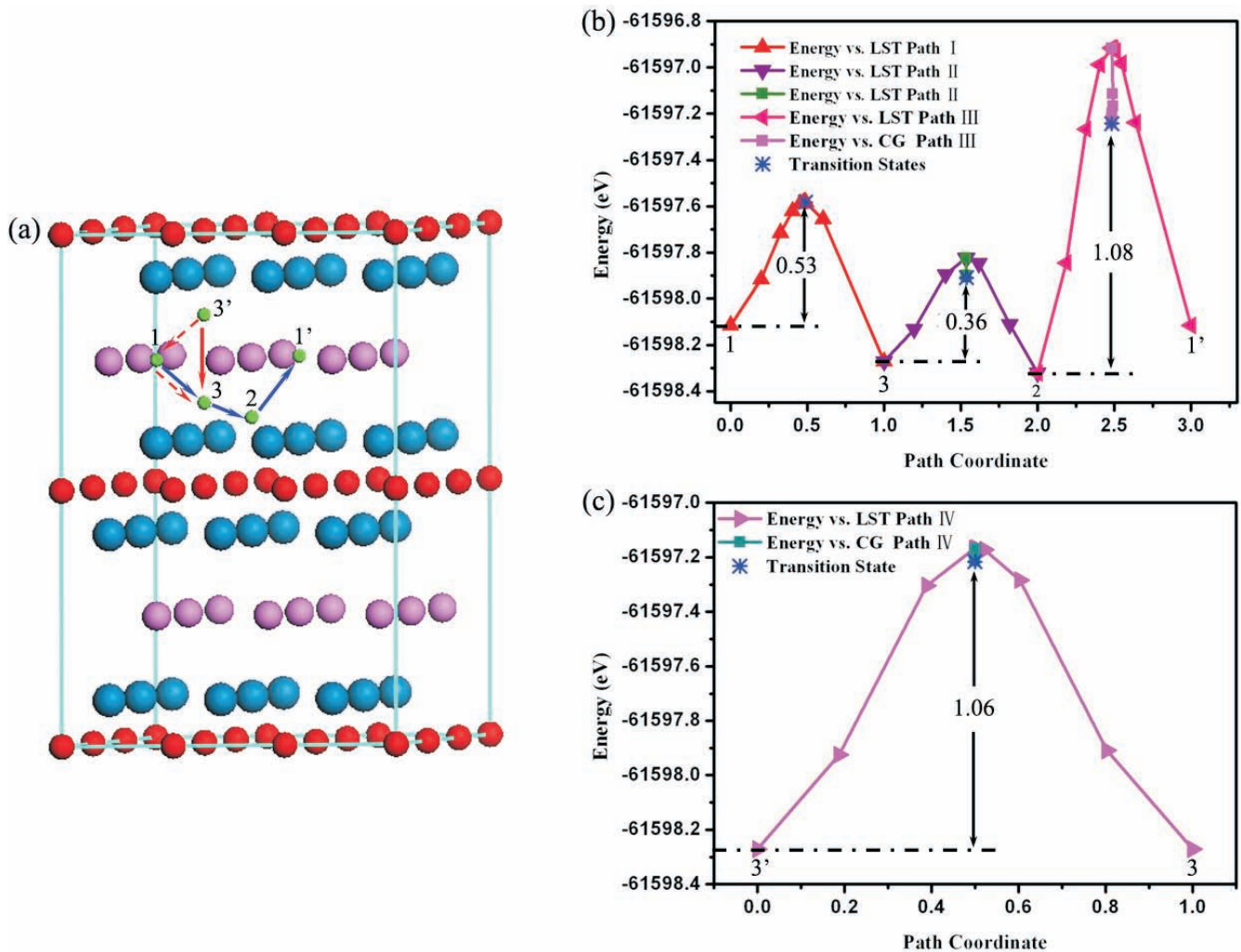


Fig. 4: The diffusion of H atoms in Ti-Al layers of Ti_2AlC (a) possible diffusion paths; (b) diffusion energy profiles and barrier energies (eV) for H diffusion along the basal plane; (c) diffusion energy profiles and barrier energies (eV) for H diffusion along the c-axis.

IV. Conclusions

In summary, first-principles calculations have been performed to study hydrogen insertion in Ti_2AlC and its influence on the crystal structure and bonds. It is found that H insertion into interstitial sites of Ti-Al layers including the tetrahedral interstitial sites ($I_{tetra-2}$) surrounded by three Ti atoms and one Al atom, the octahedral interstitial sites (I_{oct-3}) surrounded by three Ti atoms and three Al atoms, and the hexagonal interstitial sites (I_{hexa-5}) surrounded by three Al and two Ti atoms is thermally favorable. When H atoms are inserted into $I_{tetra-2}$, the surrounding Ti-Al bonds will be substituted by H-Al and H-Ti bonds. When H atoms are inserted into I_{hexa-5} , the strength of the Ti-Al bonds will be weakened while H-Ti bonds will be formed, at the same time, Al-Al bonds in Al layers will be substituted by H-Al bonds, and part of the crystal structure of Al layers will also be changed accordingly. In comparison, H insertion into I_{oct-3} has the least influence on the Ti-Al bonds. As a result, H insertion into $I_{tetra-2}$ will seriously weaken the bonding between the Ti and Al layers while H insertion into I_{hexa-5} and I_{oct-3} will enhance it. Therefore, it is considered that the influence of H on properties of Ti_2AlC closely depends on its insertion position. The LST optimization study shows that H

diffusion along the basal plane in the Ti-Al layers is feasible, while the diffusion along the c-axis is difficult.

This work was supported by the National Nature Science Foundation of China (No. 51301068), the Natural Science Foundation of Hebei Province (No. E2014502003) and the Fundamental Research Funds for the Central Universities (No. 2016MS112).

References

- Barsoum, M.W., EI-Raghy, T.: Synthesis and characterization of a remarkable ceramic: Ti_3SiC_2 , *J. Am. Ceram. Soc.*, **79**, 1953–1956, (1996).
- Bentzel, G.W., Ghidui, M., Anasori, B., Barsoum, M.W.: On the interactions of Ti_2AlC , Ti_3AlC_2 , Ti_3SiC_2 and Cr_2AlC with silicon carbide and pyrolytic carbon at 1300 °C, *J. Eur. Ceram. Soc.*, **35**, 4107–4114, (2015).
- Wang, K., Zhou, Y.F., Yu, C., Xiang, M., Huang, D.C., Xu, W.T.: Synthesis and strengthening of Ti_3AlC_2 by doping with carbon nanotubes, *J. Alloy. Compd.*, **654**, 120–125, (2016).
- Zhou, Y.C., Sun, Z.M.: Temperature fluctuation/hot pressing synthesis of Ti_3SiC_2 , *J. Mater. Sci.*, **35**, 4343–4346, (2000).
- Zhang, H.B., Hu, C.F., Sato, K., Grasso, S., Estili, M., Guo, S.Q., Morita, K., Yoshida, H., Nishimura, T., Suzuki, T.S., Barsoum, M.W., Kimb, B.N., Sakka, Y.: Tailoring Ti_3AlC_2 ceram-

- ic with high anisotropic physical and mechanical properties, *J. Eur. Ceram. Soc.*, **35**, 393–397, (2015).
- 6 Wang, X.H., Zhou, Y.C.: Oxidation behavior of Ti_3AlC_2 at 1000–1400 °C in air, *Corros. Sci.*, **45**, 891–907, (2003).
 - 7 Lin, Z.J., Li, M.S., Wang, J.Y., Zhou, Y.C.: Influence of water vapor on the oxidation behavior of Ti_3AlC_2 and Ti_2AlC , *Scripta Mater.*, **58**, 229–232, (2008).
 - 8 Wang, X.H., Li, F.Z., Chen, J.X., Zhou, Y.C.: Insights into high temperature oxidation of Al_2O_3 -forming Ti_3AlC_2 , *Corros. Sci.*, **58**, 95–103, (2012).
 - 9 Ma, J.Q., Hao, J.Y., Fu, L.C., Qiao, Z.H., Yang, J., Liu, W.M., Bi, Q.L.: Intrinsic self-lubricity of layered Ti_3AlC_2 under certain vacuum environment, *Wear*, **297**, 824–828, (2013).
 - 10 Riley, D.P., Kisi, E.H.: The design of crystalline precursors for the synthesis of $M_{n+1}AX_n$ phases and their application to Ti_3AlC_2 , *J. Am. Ceram. Soc.*, **90**, 2231–2235, (2007).
 - 11 Li, Z.M., Luo, F., He, C.C., Yang, Z., Li, P.X., Hao, Y.: Improving the microwave dielectric properties of Ti_3SiC_2 powders by Al doping, *J. Alloy. Compd.*, **618**, 508–511, (2015).
 - 12 Wu, E.D., Wang, J.Y., Zhang, H., Zhou, Y.C., Sun, K., Xue, Y.J.: Neutron diffraction studies of $Ti_3Si_{0.9}Al_{0.1}C_2$ compound, *Mater. Lett.*, **59**, 2715–2719, (2005).
 - 13 Zhang, H.B., Zhou, Y.C., Bao, Y.W., Li, M.S.: Improving the oxidation resistance of Ti_3SiC_2 by forming a $Ti_3Si_{0.9}Al_{0.1}C_2$ solid solution, *Acta Mater.*, **52**, 3631–3637, (2004).
 - 14 Xu, X.L., Ngai, T.L., Li, Y.Y.: Synthesis and characterization of quaternary $Ti_3Si_{(1-x)}Al_xC_2$ MAX phase materials, *Ceram. Int.*, **41**, 7626–7631, (2015).
 - 15 Cabioch, T., Eklund, P., Mauchamp, V., Jaouen, M., Barsoum, M.W.: Tailoring of the thermal expansion of $Cr_2(Al_x, Ge_{1-x})C$ phases, *J. Eur. Ceram. Soc.*, **33**, 897–904, (2013).
 - 16 Aryal, S., Sakidja, R., Ouyang, L.Z., Ching, W.Y.: Elastic and electronic properties of $Ti_2Al(C_xN_{1-x})$ solid solutions, *J. Eur. Ceram. Soc.*, **35**, 3219–3227, (2015).
 - 17 Xiao, J.R., Wang, C.X., Yang, T.F., Kong, S.Y., Xue, J.M., Wang, Y.G.: Theoretical investigation on helium incorporation in Ti_3AlC_2 , *Nucl. Instrum. Meth. B*, **304**, 27–31, (2013).
 - 18 Zhang, H.F., Yao, B.D., Shi, L.Q., O'Connor, D.J., Huang, J., Zhang, J.Y., Ding, W., Wang, Y.X.: Roles of silicon-layer in Ti_3SiC_2 materials response to helium irradiation: New insights from first-principles calculation, *Acta Mater.*, **97**, 50–57, (2015).
 - 19 Jia, L.X., Wang, Y.X., Ou, X.D., Shi, L.Q., Ding, W.: Decohesion of Ti_3SiC_2 induced by He impurities, *Mater. Lett.*, **83**, 23–26, (2012).
 - 20 Zhang, H.F., Yao, B.D., Zhang, J.Y., Xu, Q., Feng, Y.J., Wang, Y.X.: The tolerance of Ti_3SiC_2 to hydrogen-induced embrittlement: A first principles calculation, *Mater. Lett.*, **166**, 93–96, (2016).
 - 21 Ou, X.D., Wang, Y.X., Shi, L.Q., Ding, W., Wang, M., Zhu, Y.S.: Effect of hydrogen-doping on bonding properties of Ti_3SiC_2 , *Physica B*, **406**, 4460–4465, (2011).
 - 22 Ding, H.M., Glandut, N., Fan, X.L., Liu, Q., Shi, Y., Jie, J.C.: First-principles study of hydrogen incorporation into the MAX phase Ti_3AlC_2 , *Int. J. Hydrogen Energy*, **41**, 6387–6393, (2016).
 - 23 Arya, A., Carter, E.A.: Structure, bonding, and adhesion at the $TiC(100)/Fe(110)$ interface from first principles, *J. Chem. Phys.*, **118**, 8982–96, (2003).
 - 24 Vekilova, O.Y., Bazhanov, D.I., Simak, S.I., Abrikosov, I.A.: First-principles study of vacancy-hydrogen interaction in Pd, *Phys. Rev. B*, **80**, 024101, (2009).
 - 25 Bouhemadou, A., Khenata, R., Chegaar, M.: Structural and elastic properties of Zr_2AlX and Ti_2AlX ($X = C$ and N) under pressure effect, *Eur. Phys. J. B*, **56**, 209–215, (2007).
 - 26 Chris, G., Walle, V.D., Neugebauer, J.: First-principles surface phase diagram for hydrogen on GaN surfaces, *Phys. Rev. Lett.*, **88**, 066103, (2002).
 - 27 Govind, N., Petersen, M., Fitzgerald, G., King-Smith, D., Andzelm, J.: A generalized synchronous transit method for transition state location, *Comput. Mater. Sci.*, **28**, 250–258, (2003).
 - 28 Wang, C.X., Yang, T.F., Xiao, J.R., Liu, S.S., Xue, J.M., Wang, J.Y., Huang, Q., Wang, Y.G.: Irradiation-induced structural transitions in Ti_2AlC , *Acta Mater.*, **98**, 197–205, (2015).
 - 29 Wang, X.H., Zhou, Y.C.: Layered machinable and electrically conductive Ti_2AlC and Ti_3AlC_2 ceramics: A review, *J. Mater. Sci. Technol.*, **26**, 385–416, (2010).
 - 30 Xie, J., Wang, X.H., Li, A.J., Li, F.Z., Zhou, Y.C.: Corrosion behavior of selected $M_{n+1}AX_n$ phases in hot concentrated HCl solution: effect of A element and MX layer, *Corros. Sci.*, **60**, 129–135, (2012).
 - 31 Chang, F.Y., Li, C.S., Yang, J., Tang, H., Xue, M.Q.: Synthesis of a new graphene-like transition metal carbide by de-intercalating Ti_3AlC_2 , *Mater. Lett.*, **109**, 295–298, (2013).
 - 32 Medvedeva, N.I., Ivanovsky, A.L., Kuznetsov, M.V., Novikov, D.L., Freeman, A.J.: Electronic properties of Ti_3SiC_2 -based solid solutions, *Phys. Rev. B*, **58**, 16042, (1998).
 - 33 Medvedeva, N.I., Freeman A.J.: Cleavage fracture in Ti_3SiC_2 from first-principles, *Scripta Mater.*, **58**, 671–674, (2008).
 - 34 Bao, Y.W., Chen, J.X., Wang, X.H., Zhou, Y.C.: Shear strength and shear failure of layered machinable Ti_3AlC_2 ceramics, *J. Eur. Ceram. Soc.*, **24**, 855–860, (2004).
 - 35 Han, X.L., Wang, Q., Sun, D., Sun, T., Guo, Q.: First-principles study of hydrogen diffusion in alpha Ti, *Int. J. Hydrogen Energy*, **34**, 3983–3987, (2009).
 - 36 Wasilewski, R.J., Kehl, G.L.: Diffusion of hydrogen in titanium, *Metallurgia*, **50**, 225–30, (1954).
 - 37 Papazoiglou, T.P., Hepworth, M.T.: Diffusion of hydrogen in α -titanium, *Trans. Met. Soc. AIME*, **242**, 682–687, (1968).

